

Surface micelles of semifluorinated alkanes in Langmuir–Blodgett monolayers†

Guifang Zhang, Mounir Maaloum, Pierre Muller, Nicole Benoit and Marie Pierre Krafft*

Institut Charles Sadron (UPR CNRS 22) 6, rue Boussingault, 67083 Strasbourg, France.
E-mail: krafft@ics.u-strasbg.fr; Fax: +33 3 88 40 41 99; Tel: +33 3 8 41 40 60

Received 17th November 2003, Accepted 10th February 2004
First published as an Advance Article on the web 1st March 2004

We have studied the molecular patterns formed in Langmuir–Blodgett (LB) films of semifluorinated alkanes $C_nF_{2n+1}C_mH_{2m+1}$ (*FnHm* diblocks, $n = 6, 8, 10, m = 14, 16, 18, 20$) by atomic force microscopy. All the compounds investigated formed surface micelles whose shape and dimensions varied with the molecular structure of the *FnHm* diblocks. Except for F6H16 and F8H14, which produced exclusively circular micelles, all of the other diblocks also formed elongated micelles that coexisted with circular micelles. The mean diameter of the circular micelles increased with the length of the hydrogenated segment of the diblocks. By contrast, increasing the length of the fluorinated segments did not have any detectable effect on the diameter. The elongated micelles became more numerous and longer for longer *FnHm* (both the length of the hydrogenated and of the fluorinated segments had a strong effect). The surface pressure of transfer had an influence on the morphology of the elongated micelles, the latter becoming fewer and shorter for higher surface pressures. A detailed X-ray reflectivity study conducted on F8H16 LB films showed that the hydrogenated segments are directed towards the silicon wafer, while the fluorinated segments point outwards toward the air. A disc-like model is proposed for the surface micelles.

Introduction

Colloidal systems involving semifluorinated alkanes $C_nF_{2n+1}C_mH_{2m+1}$ (*FnHm* diblocks) have recently focussed attention owing to their potential applications in the biological and materials sciences.^{1,2} These nonpolar, nonetheless amphiphilic molecules were shown to impart specific properties (increased stability, reduced permeability, reduced fusion rate, *etc.*) to various colloidal systems of biological interest including vesicles (liposomes),^{3,4} fluorocarbon-in-water emulsions^{5,6} and hydrocarbon-in-fluorocarbon emulsions.⁷ One of our objectives is to exploit the mutual antipathy between fluorinated and hydrogenated chains for the elaboration of nanopatterned surfaces.⁸ Compression of Langmuir monolayers and Langmuir–Blodgett (LB) films of combinations of *FnHm* diblocks and phospholipids provided evidence for both lateral and vertical phase separation.^{9,10} Precise control of the shape, size and molecular organization of the molecular clusters decorating the solid substrates is necessary to achieve mastered construction of 2D supramolecular architectures.

Despite several studies conducted on Langmuir monolayers of semifluorinated alkanes,^{11–13} the molecular orientation of the diblock molecules at the air/water interface has remained controversial. We present here an investigation by atomic force microscopy (AFM) of the morphology of Langmuir monolayers of a series of *FnHm* diblocks ($n = 6, 8, 10$ and $m = 14, 16, 18, 20$) after transfer onto silicon wafers. The AFM images were analyzed using an image analysis software (Visilog®).

Experimental section

Materials

FnHm diblocks were synthesized according to ref. 14 and were thoroughly purified by repeated crystallization from acetone.

Their purity (>99%) was determined by TLC, NMR and elemental analysis. Spreading solutions of *FnHm* (1 mmol L⁻¹) were prepared in chloroform (analytical grade). Water was purified using a Millipore system (surface tension: 72.1 mN m⁻¹ at 20 °C, resistivity: 18.2 MΩ cm).

Monolayer isotherms–monolayer transfer

Surface pressure *versus* molecular area (π – A) isotherms were recorded on a Langmuir minitrough (Riegler & Kirstein, Germany) equipped with two movable barriers (compression speed: 0.1 nm² min⁻¹). The surface pressure π was measured using the Wilhelmy plate method. Temperature was regulated at 20.0 ± 0.5 °C. 25 μL of *FnHm* solution were spread on the water surface and 5 min were allowed for solvent evaporation.

The monolayers were compressed up to the desired surface pressure and transferred onto a silicon wafer treated with piranha solution (conc. H₂SO₄ + 30% H₂O₂ 3:1), using the LB technique (one monolayer transferred, lift speed of 5 mm min⁻¹).

AFM images–X-ray reflectivity

The transferred films were analyzed with an atomic force microscope (NanoScope III) in tapping mode. The cantilever (Olympus) was fitted with a very sharp tip (5 nm). The resonance frequency was 300 kHz and the spring constant 42 mN m⁻¹. The digitized AFM images were analyzed with Visilog® Image Analysis Software (Noesis, France) using filtering techniques, a morphological gradient method, mathematical morphology functions, and adaptive thresholding.¹⁵

The grazing incidence X-ray studies of the transferred films of F8H16 were performed with an EXPERT-MPD device from Philips (divergence slit 1/32°, parallel plate collimator, flat Ge monochromator and Xe detector). A Cu K α beam at wavelength 0.1542 nm was used. The data were analyzed using Parratt32 software (version 1.6.0).¹⁶

† Presented at the 17th Conference of the European Colloid and Interface Society, Firenze, Italy, 21–26 September 2003.

Results and discussion

1. Surface pressure–molecular area (π - A) compression isotherms of F_nH_m diblocks

The isotherms of the F_nH_m diblocks investigated indicate that, except for F6H16, the shortest diblock, which is also the less fluorinated one, all the other diblocks form stable Langmuir monolayers (Fig. 1), as shown in ref. 11. The longer the F_nH_m molecule, the higher the surface pressure of collapse, π^c . Moreover, by comparing two diblocks of same length, the most fluorinated one gave the most stable monolayer. For example, F10H16 had a higher π^c ($\sim 22 \text{ mN m}^{-1}$) than F8H18 ($\sim 15 \text{ mN m}^{-1}$). All the monolayers formed by the F_nH_m diblocks (except F6H16) had a similar extrapolated molecular area of about 0.31 nm^2 , corresponding to the cross-section of a perfluorinated chain, which is larger than the cross-section of a typical hydrogenated chain (*ca.* 0.20 nm^2).¹⁷ Because the van der Waals radius of fluorine is larger than half the C–C bond distance, steric hindrance causes the chain to adopt a (15/7) helical conformation, and renders the carbon backbone rigid.¹⁸ The isotherms were reversible, without hysteresis, upon compression–expansion cycles.

2. Influence of the F_nH_m molecular structure on the shape of the micelles: circular vs. elongated

The monolayers of F_nH_m diblocks were investigated by AFM after transfer onto silicon wafers. All the F_nH_m diblocks formed surface micelles. Two-dimensional surface micelles have been visualized by AFM in monolayers of partially fluorinated carboxylic acids spread on a cadmium acetate subphase and transferred on cover glass.¹⁹ The shape and dimensions of the F_nH_m surface micelles varied with the molecular structure of the diblock. As illustrated in Fig. 2, some diblocks, *e.g.* F8H16, led principally to circular micelles, while in the AFM images of other diblocks (*e.g.* F8H20), elongated micelles that coexisted with circular micelles were clearly visible. The variation of the sum area fraction of the long micelles, as determined by the image analysis software Visilog[®], is plotted on Fig. 3a–c as a function of the lengths of the F_n and H_m segments and of the total length of the diblock molecule. The monolayers were transferred at 5 mN m^{-1} . The results showed that the area fraction of the elongated micelles increased from 0 to 10% with the length of the diblock molecule. Both the lengths of F_n and H_m segments had a strong effect. Further studies are presently underway to determine whether the shape of the micelles is changing from circular to elongated, or whether circular domains coalesce to form elongated domains.

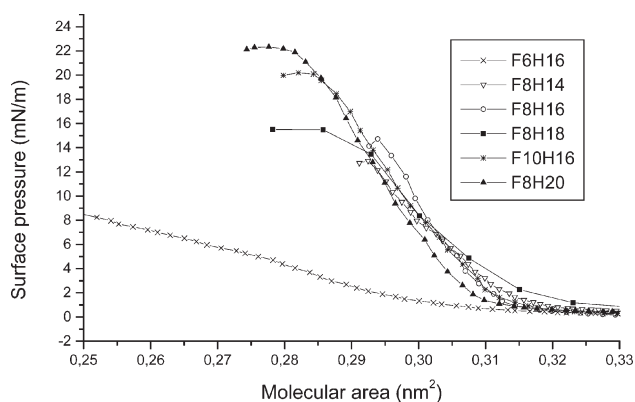


Fig. 1 Surface pressure–molecular area (π - A) compression isotherms of F_nH_m diblocks at the air/water interface at 20°C .

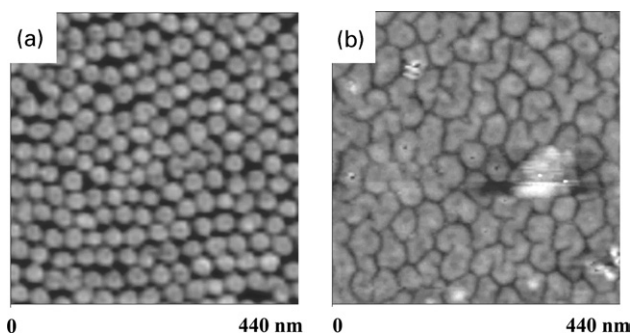


Fig. 2 AFM images of LB films of (a) F8H16 and (b) F8H20 transferred onto silicon wafers at 5 mN m^{-1} . While circular surface micelles are almost exclusively observed for F8H16, a significant amount of elongated, snake-like surface micelles is present in the films of F8H20.



Scheme 1 Schematic representation (disk-like model) of the cross-section of a surface micelle of F8H16 after transfer of the monolayer onto a silicon wafer. The black area represents the fluorinated segment F8 region and the dotted area represents the hydrogenated segment H16 region.

3. X-ray reflectivity study of F8H16 LB films

Although F6H16 and F8H14 exclusively produced circular micelles (Fig. 2), they did not lead to LB films stable enough to carry out an X-ray analysis. F8H16 was therefore selected for this study because of the stability of its LB films, and because it led to a monodisperse population of circular micelles with only a very limited number of long micelles (fraction area of $\sim 3\%$). The F8H16 monolayer, compressed at 7 mN m^{-1} , was analyzed by X-ray specular reflectivity after transfer onto a silicon wafer.¹⁹ The experimental curve was fitted with a two-layer model that provided an excellent agreement with the data. The electron density distribution of the two-layer model (Fig. 4) consisted of an upper layer with a thickness of 1.0 nm and an electron density of 487 e nm^{-3} (a fluorinated layer) and of a lower layer with a thickness of 1.93 nm and an electron density of 290 e nm^{-3} (a hydrogenated layer). The total thickness of the monolayer was 2.93 nm , close to the length of a fully extended F8H16 molecule (3.32 nm). These results definitely demonstrate that the hydrogenated segments of the F8H16 molecules are directed toward the substrate, while the fluorinated segments are pointing outwards toward air. Altogether, the results of the AFM and X-ray reflectivity showed that the size of the surface micelles is controlled by the density mismatch between the fluorinated and hydrogenated segments. A disc-like shape model was proposed for the circular micelles formed by F8H16 (Scheme 1).²⁰

4. Influence of the F_nH_m molecular structure on the dimensions of the surface micelles

a. **Diameter of the circular micelles.** Fig. 5a–c displays the variations of the mean diameter of the circular micelles as a function of the lengths of F_n , H_m , and of the overall molecule. The monolayers of F_nH_m diblocks were transferred at 5 mN m^{-1} . It is noteworthy that, for a given length of the H_n segment, increasing the length of the F_n segment did not significantly influence the diameter of the micelles (Fig. 5a).²¹ On the other hand, the diameter of the circular micelles increased strongly with the H_m segment length for a given F_n length (Fig. 5b). As a consequence, for a given carbon number, increasing the weight of the fluorinated part of the F_nH_m diblocks resulted in a decrease of the size of the micelles (Fig. 5c).

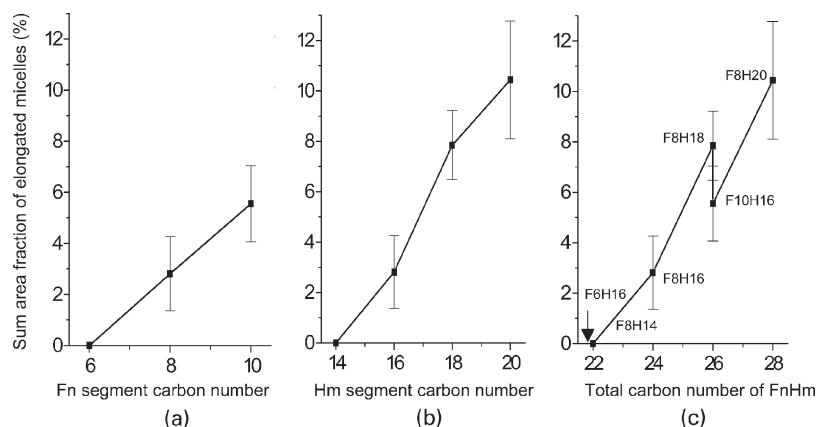


Fig. 3 Variation of the area fraction of elongated micelles in LB films of F_nH_m as a function (a) of the length of the F_n segment (for a constant H16 segment), (b) of the length of the H_m segment (for a constant F8 segment), and (c) of the overall length of the F_nH_m molecule.

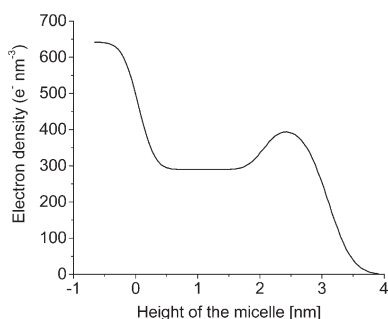


Fig. 4 Variation of the electron density as a function of the height of the circular micelles corresponding to the fit of the experimental reflectivity curve of the F8H16 monolayer.

b. Length of the elongated micelles. Fig. 6a–c displays the variations of the length of the elongated micelles, as determined by Visilog[®], as a function of the length of the F_n segment, the length of the H_m segment, and the overall length of the F_nH_m molecule. It can be seen that the longer the H_m segment and/or F_n segment, the longer the elongated micelles. It is noteworthy that both the hydrogenated and fluorinated segments have an impact on the length of the elongated micelles.

5. Influence of the surface pressure of transfer on the elongated micelles

Although the surface pressure of transfer, π_t , of the monolayer onto the silicon wafer had no significant influence on

the diameter of the circular micelles,²¹ it had a substantial impact on the morphology of the long micelles. The higher π_t , the smaller the area fraction of the elongated micelles. This was observed for both the sum area fraction (Fig. 7) and for the average area fraction of one single domain (data not shown). It was also observed that the higher π_t , the shorter the length of the elongated micelles (Fig. 8). This suggests that the elongated micelles are transformed into circular micelles at high π_t , providing a more regular arrangement. The long micelles may either break or curl to rearrange into circular micelles.

Conclusions

We have demonstrated that monolayers of semifluorinated alkanes $C_nF_{2n+1}C_mH_{2m+1}$ (F_nH_m , $n = 6, 8, 10$, $m = 14, 16, 18, 20$) transferred onto silicon wafers consist of surface micelles. The shape of the micelles, circular or elongated, depends on the F_nH_m molecular structure; the longer the H_m segment, the larger the diameter of the circular micelles. By contrast, the length of the F_m segment does not influence the diameter significantly. The elongated micelles are more numerous and longer for the longer F_nH_m , both the F_n and H_m segments having a strong effect. The surface pressure of transfer influences the shape and the length of the elongated micelles; the higher the surface pressure, the smaller their area fraction and the shorter their length. This work implicates that semifluorinated alkanes may be used to decorate surfaces with molecular clusters of controlled shape and predetermined size in the nanometer range.

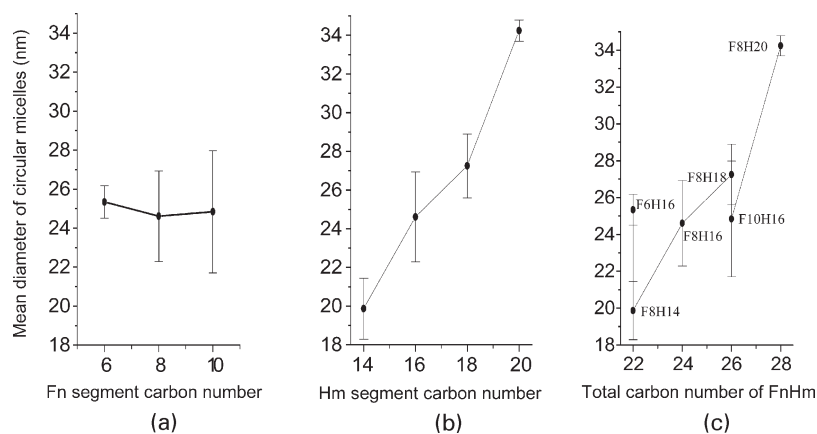


Fig. 5 Variation of the mean diameter of the circular surface micelles of F_nH_m as a function (a) of the length of the F_n segment (for a constant H16 segment), (b) of the length of the H_m segment (for a constant F8 segment), and (c) of the overall length of the F_nH_m molecule.

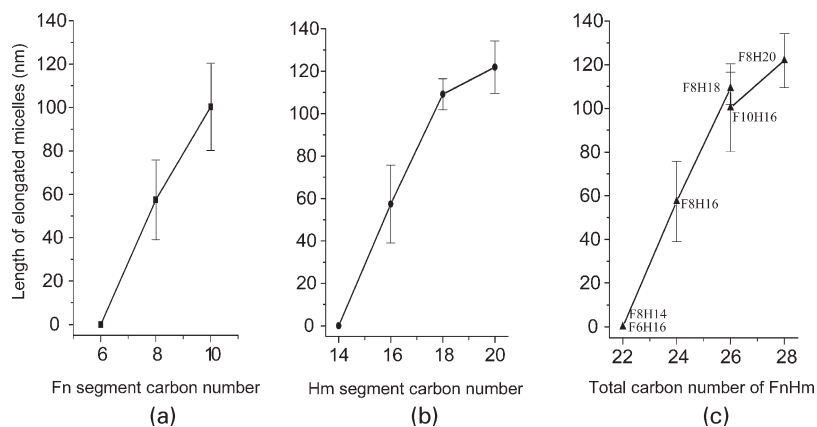


Fig. 6 Variation of the length of the elongated micelles of F_nH_m as a function (a) of the length of the F_n segment (for a constant H16 segment), (b) of the length of the Hm segment (for a constant F8 segment), and (c) of the length of the overall F_nH_m molecule.

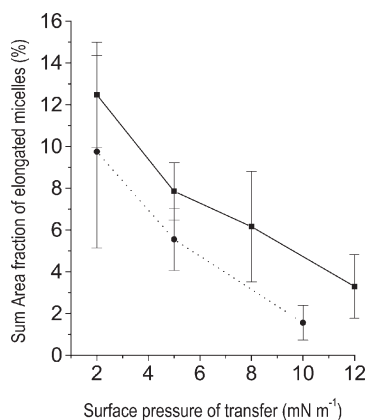


Fig. 7 Variation of the sum area fraction of the elongated micelles of F8H18 (solid line) and F10H16 (dotted line) as a function of the surface pressure of transfer.

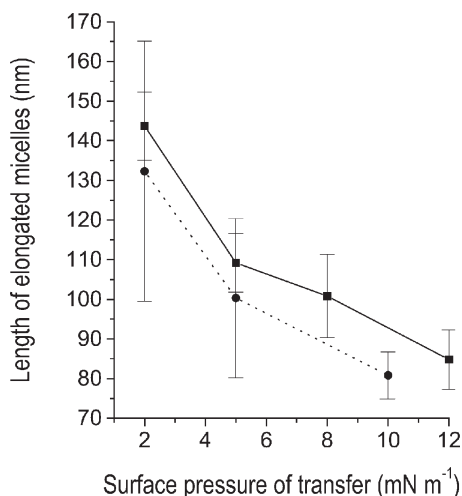


Fig. 8 Variation of the length of the elongated micelles of F8H18 (solid line) and of F10H16 (dotted line) as a function of the surface pressure of transfer.

Acknowledgements

We wish to thank Prof. J. G. Riess for useful discussions. GF Zhang thanks the French Minister of Research for a Post-Doctoral Fellowship. We also acknowledge AtoFina for the gift of fluorinated precursors and the Centre National de la Recherche Scientifique (CNRS) for financial support.

References

- 1 J. G. Riess, *Tetrahedron*, 2002, **58**, 4113–4131.
- 2 P. Lo Nostro, *Curr. Opin. Colloid Interface Sci.*, 2003, **8**, 223–226.
- 3 Y. Ferro and M. P. Krafft, *Biochim. Biophys. Acta*, 2002, **1581**, 11–20.
- 4 M. Schmutz, B. Michels, P. Marie and M. P. Krafft, *Langmuir*, 2003, **19**, 4889–4894.
- 5 J. G. Riess, *Chem. Rev.*, 2001, **101**, 2797–2919.
- 6 S. Marie Bertilla, J. L. Thomas, P. Marie and M. P. Krafft, *Langmuir*, 2004, in press.
- 7 M. P. Krafft, L. Dellamare, T. Tarara, J. G. Riess and L. Trevino, WO97/21425 (June 19, 1997).
- 8 M. Krafft and M. Goldmann, *Curr. Opin. Colloid Interface Sci.*, 2003, **8**, 243–250.
- 9 M. P. Krafft, F. Giulieri, P. Fontaine and M. Goldmann, *Langmuir*, 2001, **17**, 6577–6584.
- 10 M. Maaloum, P. Muller and M. P. Krafft, *Langmuir*, 2004, 10.1021/la030312q.
- 11 G. L. Gaines, *Langmuir*, 1991, **7**, 3054–3056.
- 12 Z. Huang, A. A. Acero, N. Lei, S. A. Rice, Z. Zhang and M. L. Schlossman, *J. Chem. Soc. Faraday Trans.*, 1996, **92**, 545–552.
- 13 A. El-Abed, E. Pouzet, M.-C. Fauré, M. Sanière and O. Abillon, *Phys. Rev. E*, 2000, **62**, R5895–R5898.
- 14 N. O. Brace, *J. Org. Chem.*, 1973, **38**, 3167–3172.
- 15 M. Coster and J. L. Chermant, *Précis d'Analyse d'Images*, Presses du CNRS, Paris, 1989.
- 16 C. Braun, *Parratt32 Fitting routine for reflectivity data*, Hahn–Meitner Institut, Berlin, 1997–1999.
- 17 A. Acero, M. Li, B. Lin, S. Rice, M. Goldmann, I. Azouz, A. Goudot and F. Rondelez, *J. Chem. Phys.*, 1993, **99**, 7214.
- 18 C. W. Bunn and E. R. Howells, *Nature*, 1954, **174**, 549.
- 19 T. Kato, M. Kameyama, M. Ehara and K.-I. Imura, *Langmuir*, 1998, **14**, 1786.
- 20 M. Maaloum, P. Muller and M. P. Krafft, *Angew. Chem., Int. Ed. Engl.*, 2002, **41**, 4331–4334.
- 21 G. F. Zhang, M. Maaloum, P. Marie, P. Muller, N. Benoit and M. P. Krafft, in preparation.